BULETINUL INSTITUTULUI POLITEHNIC DIN IAŞI
Publicat de
Universitatea Tehnică „Gheorghe Asachi” din Iaşi
Volumul 65 (69), Numărul 1, 2019
Secţia
CHIMIE şi INGINERIE CHIMICĂ

SYNTHESIS, CHARACTERIZATION AND TOXICITY ANALYSIS OF SOME DIVALENT TRAZITIONAL METALS COMPLEXES WITH N-(p-NITROBENZOYL)-L-GLYCINE

BY

CĂTĂLINA ROȘCA[1], VALERIU ȘUNEL[2], MIHAELA CREȚU[2], MARIANA DIACONU[1], BOGDAN ISTRATE[3], GABRIELA LISĂ[1], MIHAI IMBRIȘCĂ[1], CORNELIU STAN[1], GABRIELA ANTOANETA APOSTOLESCU[1] and DANIEL SUTIMAN[1,*]

[1]“Gheorghe Asachi” Technical University of Iași, Romania,
“Cristofor Simionescu” Faculty of Chemical Engineering and Environmental Protection
[2]“Alexandru Ioan Cuza” University of Iași, Romania,
Faculty of Chemistry
[3]“Gheorghe Asachi” Technical University of Iași, Romania,
Faculty of Mechanical Engineering

Received: December 15, 2018
Accepted for publication: January 26, 2019

Abstract. This paper presents the synthesis, structural and physico-chemical characterization of Mn(II), Co(II), Ni(II) and Cu(II) complexes with N-(p-nitrobenzoyl)-L-glycine as ligand. Firstly, four complexes were synthesized in 1:2 molar ratio, followed by their characterization and determination of their toxic potential (toxicity lethal dose) as well analysis of some antifungal and antibacterial properties. The characterization step involved the structure investigation by elemental analysis, FTIR spectroscopy, XRD, ESR and the thermal stability. Experimental data shows that all compounds have a crystalline structure (orthorhombic system) and are thermally stable up to temperatures above 100°C. Toxicity tests of new compounds were run on mice and the results indicate that the lowest value of the lethal dose is displayed by the copper compound. The biological and antifungal activities were investigated for all

[*]Corresponding author; *e-mail*: sutiman@ch.tuiasi.ro

compounds, the cobalt compound displays the best antibacterial properties and the copper compound presents the best antifungal properties.

Keywords: divalent transitional metals complexes; N-(p-nitrobenzoyl)-L-glycine; XRD; FTIR; ESR; antibacterial and antifungal activity.

1. Introduction

There are many heterocyclic compounds with various applications in medicine and pharmacology due to various effects they have on the human body and other living organisms. Some antifungal (Chen *et al*., 2000; Zamani *et al*., 2004; Zan *et al*., 2002) and antibacterial (Gokce *et al*., 2001; Pintilie *et al*., 2007a; Varvarason *et al*., 2000) effects are known. A series of N-acylated amino acids occur as hepato-protective, antimicrobial and antitumoral (Moise *et al*., 2008; Pintilie *et al*., 2007b; Șunel *et al*., 2002; Șunel *et al*., 2005; Șunel *et al*., 2008).

Due electron donation properties and functional groups capable of forming coordination bonds, some amino acids or their derivatives have been used as ligands for the synthesis of complex combinations (Ryabov *et al*., 1984; Gudasi *et al*., 2007; Pelagatti *et al*., 2005; Salas Peregrin *et al*., 1985; Inomata *et al*., 1988;).

In this paper we present the synthesis and characterization of four coordination compounds of Mn(II), Co(II), Ni(II) and Cu(II) with N-(p-nitrobenzoyl)-L-glycine (L).

The organic ligand was synthesized at 10-12^{o}C by condensation reaction between chloride of p-nitrobenzoyc acid (dissolved in anhydrous benzene) with glycine, into a solution of sodium bicarbonate.

The product was purified by column chromatography on silica gel using as eluent a mixture of dichloromethane-methanol 9:2 (Pintilie *et al*., 2006). The ligand structure is shown in Fig. 1.

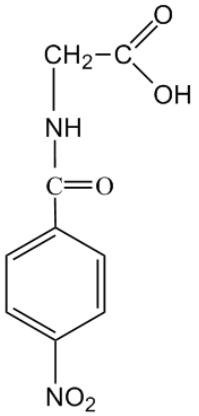

Fig. 1 – Structure of N-(p-nitrobenzoyl)-L-glycine.

2. Experimental Part

Complexes were synthesized by direct reaction between a 0.1 M solution of ligand dissolved in ethanol and 0.1 M solution of metal chloride dissolved in water in a molar ratio of 2/1, stirring at 50°C for 3 h.

The final product was separated by slow crystallization at room temperature for several days, purified by recrystallization in ethanol and washed until there is no Cl^- ion by testing with $AgNO_3$.

To determine the structure of these compounds was carried out the following investigations: elemental analysis of C, N, and H by oxygen combustion and O by pyrolysis, on the Thermo Fisher Scientific equipment Flash EA-1112CHNS / O, the metal being calculated by difference. Data acquisition and interpretation was performed with specialized software - Eager 300.

FTIR analysis was performed on a Perkin-Elmer Spectrum 100 device, in the range 400-4000 cm^{-1} (in KBr), aiming at the mainly changes in group - COOH and R-NH ligand that binds to cation metal.

ESR spectra were performed on a device ESR CMS 8400, (3216.9 Gauss magnetic field corresponding to sample centre and 9030 MHz frequency). The spectroscopic splitting factor g and odd number of electrons that return each metal atom, using the standard diphenyl picryl hydrazine were determined.

XRD analysis was performed on a device Holland X'Pert diffractometer PROMRD Panalytical (Cu Kα radiation) to determine basic parameters and cell volume.

Thermal stability was analyzed on a Diamond TG / DTA (PerkinElmer) thermo-balance with a heating rate of 10°C min^{-1} in the range 20-700°C.

Toxicity tests were evaluated based on the (LD_{50}) indicator representing the dose that kills 50% of the experimental animals.

The antibacterial activities of the synthesized complexes against Gram positive bacteria *Staphylococcus aureus*, *Bacillus substilis*, Gram negative bacteria *Escherichia coli* and *Pseudomonas aeruginosa* were screened using the agar well diffusion method. The wells were making in the media using a sterile metallic borer with the centers at least 20 mm apart. Eight – hour – old bacteria inoculums containing approximately 10^6 colony forming units CFU/mL were spread on the surface of nutrient agar using sterile cotton swabs. Test compounds (2 $mg \cdot mL^{-1}$ in sterile distilled water) were introduced into the respective wells. Other wells were supplemented with sterile distilled water as a positive control. The plates were incubated at 37°C for 20 h and after this period, the activity was determined by measuring the diameter of zones showing complete inhibition (in mm). Growth inhibition was calculated with reference to positive control and also the degree of growth inhibition was calculated.

The antifungal activities of the synthesized compounds against two fungi species: *Candida albicans* and *Aspergillus fumigatus* were tested by using

the tube diffusion test. Stock solutions of synthesized compounds (100 mg·mL^{-1}) were prepared in sterile distilled water. Sabouraud dextrose agar media (10 mL) was distributed into sterile tubes and autoclaved at 121°C for 15 min. Test compounds (10 mg·mL^{-1}) were added from the stock solutions to unsolidified media. After solidification at room temperature the tubes were inoculated with 4 mm diameter portion of inoculums derivate from a seven day old fungal culture. A control tube (without test solutions) for each fungus strain was inoculated. All experimental tubes were incubated at 27°C for 5-7 days and the growth of tested fungi was determined by measuring the linear growth (in mm) in test tubes and compared to the growing of fungus in control. The degree of growth inhibition was calculated as:

Inhibition (%) = [(A-B)/B] x 100 were:

A = linear growth of fungal colony in control tube

B = linear growth of fungal colony in test tube

3. Results and Discussion

Elemental analysis

Elemental analysis data are presented in Table 1

Table 1

Theoretical and Experimental Chemical Composition of Synthesized Compounds

Complex with	% C		% N		% H		% O		% metal	
	Calc.	Exp.	Calc.	Exp.	Calc.	Exp.	Calc.	Exp.	Calc.	Exp.
Mn(II)	40.07	39.96	10.38	10.42	3.75	3.73	35.62	35.70	10.18	10.19
Co(II)	39.77	39.75	10.35	10.43	3.68	3.64	35.36	35.39	10.84	10.78
Ni(II)	39.78	39.75	10.36	10.32	3.68	3.72	35.38	35.37	10.80	10.81
Cu(II)	39.46	39.44	10.24	10.29	3.67	3.65	35.06	35.01	11.59	11.61

Theoretical calculation was made based on the molecular formula $M(L)_2(H_2O)_2$ and the analysis indicates that all compounds correspond to this formula.

FTIR spectroscopy

IR assignments of selected diagnostic bands for L (**1**) ligand and complexes (**2-5**) are given in Fig. 2 and Table 1. In the 3400-3300 cm^{-1} region, the spectrum of **1** exhibit a sharp band at 3358 cm^{-1} assigned to the O-H stretching vibration of COOH group. The IR spectra of four complexes exhibit intense and broad bands at 3484/3412 cm^{-1} (**2**), 3441 cm^{-1} (**3**), 3474 cm^{-1} (**4**), 3503/3424 cm^{-1} (**5**) attributable to the O-H stretching mode of H_2O molecule.

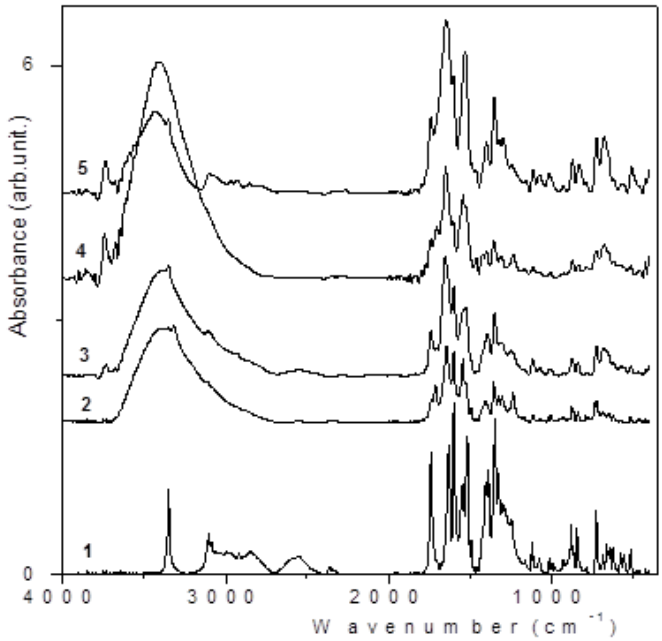

Fig. 2 − Infrared spectra of (1) L, (2) $[Mn(L)_2]\cdot 2H_2O$, (3) $[Co(L)_2]\cdot 2H_2O$, (4) $[Ni(L)_2]\cdot 2H_2O$ and (5) $[Cu(L)_2]\cdot 2H_2O$.

The broadness and frequencies of these bands are both indicative of M^{II}-OH_2 coordinative bonds. Lower intensity of ν(O-H) bands for **2** complex and presence of additional sharp band at 3562 cm^{-1} for **4** and 3582 cm^{-1} for **5** can be explained by the existence of intermolecular hydrogen bonds between water molecules and oxygen atom/atoms of neighbouring C=O groups. The corresponding deformation band, assignments of $\delta(H_2O)$ is partial overlapped by the IR strong bands from 1700-1600 cm^{-1} zone.

Table 2

Infrared Frequencies (cm^{-1}) and Assignments of Characteristic Absorption Bands for (1) L, (2) $[Mn(L)_2]\cdot 2H_2O$, (3) $[Co(L)_2]\cdot 2H_2O$, (4) $[Ni(L)_2]\cdot 2H_2O$ and (5) $[Cu(L)_2]\cdot 2H_2O$

1	2	3	4	5	Assignments
3358	3484/3412	3441	3474	3503, 3424	ν(OH) (COOH) ν(OH) (H_2O)*
3103	3323	3351	3321	3351	ν(NH)*
2993/2849	3093/2938	3094/2946	3102/2982	3106/2966	$\nu(CH)_{methyl\ (as/s)}$*
1738	1711	1738	1703	1738	$\nu_{as}(COO)$
1634	1641	1651	1647	1647	$\nu(C=O)_{amide\ I}$,
1541	1525	1526	1527	1526	$\nu_{amide\ II}$,
	1408	1389	1398	1398	$\nu_s(COO)$

*determined by deconvolution of original spectrum

The stretching vibration of N-H amide group of **1** is a relative weak band and is partial overlapped by the $\nu(CH)_{methyl}$ bands. After coordination of ligand, the ν(NH) band is overlapped by the strong absorption of $\nu(OH)(H_2O)$ band and partial by the ν(CH) one, excepting the Cu(II) complex. The values of NH stretching vibration frequency increases after coordination from 3106 cm^{-1} for free **1** to 3323 cm^{-1} for **2** and **4,** 3351cm^{-1} for **3** and **5**, respectively. The shift of ν(NH) of amide group indicates the increasing of *s* character of N-H bond as consequence of the inclusion of the nitrogen atom in a heterocyclic ring with a small number of atoms (five) and the $-I_s$ inductive effect of M^{II} Lewis acid.

The C-H stretching vibration of methyl group generates relatively broad bands in the 3100-2850 cm^{-1} region which partial hide the ν(CH) multiple bands of phenyl group. After coordination of ligand to metal cations, the ν(CH) frequency of methyl group shift to higher values (Table 2) as a consequence of modification of the electronic density on carbon atom.

The spectra show a series of very weak intensity bands in the 2800-2200 cm^{-1} zone which are characteristic to the amino acid salts and can be attributed to the combination bands of deformation vibration by Fermi resonance (Nakamoto, 1986).

In the spectral 1700-1300 cm^{-1} region are populated by many frequency values which complicate the assignment of the stretching vibration mode of carboxylate group by the $\nu(C=O)_{amide\ I}$, $\nu(C=C)_{phenyl}$, $\nu(C-N)_{amide\ II}$, δ(NH), δ(CH) modes.

The intense band at 1711 cm^{-1}, 1738 cm^{-1}, 1703 cm^{-1}, 1738 cm^{-1}, respectively in spectra of **2-5** complexes was assigned to the asymmetric stretching vibration of the carboxylate group which is overlapped with the δ(NH) and δ(OH). The four complexes also show another strong or medium intensity bands at 1408, 1389, 1398 and 1398 cm^{-1} which can be assigned to the symmetric vibration of the coordinated COO^- group that partial overlaps with CH bending frequency. The result shows that the frequency order is related by the nature of the nature of metal cation. The antisymmetric frequencies increase, the symmetric frequencies decrease, and separation between the two frequencies increases in order:

$$Mn(II) \leq Ni(II) < Cu(II) < Co(II)$$

The observed $\Delta\nu(COO)$ for complexes are 303, 305, 340 and 349 cm^{-1}, respectively. The above frequency order indicates increasing order of metal-oxygen bond since the COO^- group becomes more asymmetrical as the metal-oxygen interaction becomes stronger.

COO^- can act as unidentate or bidentate ligand but the separation frequency between $\nu_{as}(COO)$ and $\nu_s(COO)$ ($\Delta\nu(COO)$) is a mode to distinction between the two binding states (Hodgson *et al*., 1979). The Δν values suggest a unidentate interaction of carboxylato group with metal ions.

The influence of metal cations on the amide group electronic distribution is almost the same. This means that the ketonic bond becomes stronger and the amidic bond weaker.

The most important changes after the coordination of ligand to the metal take place within range 1000-400 cm^{-1} (Fig. 2). The spectra display the bands with different intensities. The position and intensity of these bands depend by the *cis* or *trans* configuration of complexes, vibration modes of ligand are strongly coupled with other skeletal modes.

As expected from symmetry consideration, the cis-isomer exhibits more bands in IR region than trans-isomer. In the low frequency region, the cis-isomer is expected to exhibit two ν(MN) and ν(MO), whereas the tran-isomer only one for each of these modes. From these reason the values of M-N and M-O vibrations is difficult to establish, but ν(M-N) appears at higher energy than ν(M-O) (Forti *et al*., 1991; Hodgson *et al*., 1979; Malek *et al*., 2004).

DR electronic spectra

Visible and near-IR spectra for solid ligand and complexes are shown in Fig. 3, and their spectral components are summarized in Table 3.

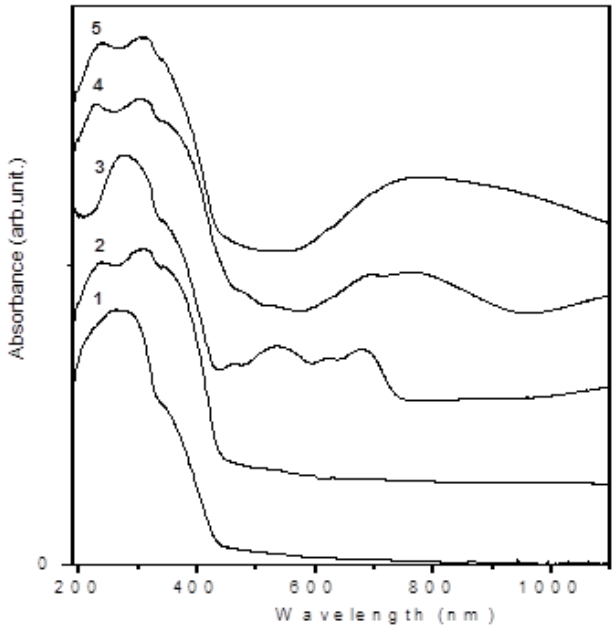

Fig. 3 − Electronic DR spectra of the (1) L, (2) $[Mn(L)_2]\cdot 2H_2O$, (3) $[Co(L)_2]\cdot 2H_2O$, (4) $[Ni(L)_2]\cdot 2H_2O$ and (5) $[Cu(L)_2]\cdot 2H_2O$.

The electronic spectrum of free L (Fig. 3) appears as an intense, asymmetric band into UV region. After Gaussian deconvolution, it was

identified four absorption bands (Table 3). These transition bands were assigned to n-π* and π-π* transitions, both types are split into two different components.

Table 3

The DR Spectral Data (λ, nm), Dq (cm^{-1}) and B (cm^{-1}) Crystal Field Parameters for (1) L, (2) $[Mn(L)_2]\cdot 2H_2O$, (3) $[Co(L)_2]\cdot 2H_2O$, (4) $[Ni(L)_2]\cdot 2H_2O$ and (5) $[Cu(L)_2]\cdot 2H_2O$

Complex	Ligand-ligand			Charge transfer		d-d			Dq, [cm^{-1}]	B*, [cm^{-1}]	
1	205	268	305	354							
2	<190	266	305	375		477	529			447	682
3	<190	243	305	373	443	535	630	688	1162	768	607
4	<190	226	297	377	647	483	692	763	1126	919	678
5	<190	234	306	374	667	-	751	882	1039	-	-

*Racah parameter

Their transition energy depends by the electronegativity of atoms and the effect of the p-nitrobenzoyl-auxochrome groups: $\nu_{n_N-\pi^*}$ = 28248 cm^{-1} (354 nm), $\nu_{n_O-\pi^*}$ = 32787 cm^{-1} (305 nm), $\nu_{\pi_C-\pi^*}$ = 37313 cm^{-1} (268 nm) and $\nu_{\pi_C-\pi^*}$ = 48780 cm^{-1} (205 nm). Absorption spectra of Mn(II), Co(II), Ni(II) and Cu(II) N-(p-nitrobenzoyl)-L-glycines show the same number of bands for each complexes (Table 3). The shift of $\nu_{n_N-\pi^*}$absorbance to lower values of energy and hypsochromic shif of π-π* transitions are atributted to the complexation behavior of N amidic towards metal cations.

The interpretation of $[M(L)_2]$ spectra could be done for the octahedral symmetry; the structure of the complexes is generated by the tetragonal distorted O_h symmetry (Fig. 4) (Forti *et al.*, 1991).

In the range 400-600 nm $[Mn(L)_2]\cdot 2H_2O$ exhibit two very weak d-d bands attributed to $^6A_{1g} - {}^4T_{1g}(G)$ (18904 cm^{-1}) and $^6A_{1g} - {}^4T_{2g}(G)$ (20964 cm^{-1}) forbidden transitions. The estimation of the crystal field strength for this compound is Dq = 447 cm^{-1} and B = 682 cm^{-1}.

For $[Co^{II}(L)_2]$ were identified four d-d transition bands at 1162 nm, 688, 630 and 535 nm, respectively, assigned to $^4E_{2g}(^4T_{2g}) - {}^4A_{2g}(^4T_{1g}(^4F))$, $(^4E_{2g}(^4T_{1g}(^4F)) - {}^4A_{2g}$ are > 1200 nm), $^4B_{2g}(^4T_{2g}) - 4A_{2g}$, $^4B_{1g}(^4A_{2g}(^4F)) - 4A_{2g}$ and $^4E_g(^4T_{1g}(^4P)) - {}^4A_{2g}$. The intensity of electronic transition bands and the gap between them allow to made distinction between pseudo-square planar and octahedral symmetry of coordinative center.

The result of Gaussian deconvolution is typical for a distorted octahedral Ni(II)-d^8 coordinative compounds (Table 1). The λ_{d-d} determined were assigned to $^3T_{2g}(F) - {}^3A_{2g}$ (1126 nm), $^3T_{1g}(F) - {}^3A_{2g}$ (763 nm),$^3T_{1g}(P) - {}^3A_{2g}$ (483 nm) spin-allowed transitions and $^1E_g - {}^3A_{2g}$ (692 nm) spin-forbidden transition. Probable, the higher energy states interact more with the larger and more polarizable N-donor atom than with the oxygen atom of L ligand. This is

equivalent with a vibronically induced electronic transition of all four band transitions and a tetragonal distorsion in the excitated states.

For Co(II) and Ni(II) complexes the Dq and B values of crystal field parameters indicate an increase of strength of ligand field and the covalent character of metal-ligand bonds, respectively, compared with the Mn(II) spectral data.

The broad band is characteristic for distorted octahedral Cu(II) complexes to CuN_2O_2 chromophore plane and spin-orbital coupling coefficient of Cu(II) (> 800 cm^{-1}). The number and energy of d-d electronic transitions of Cu(II) are influenced by the polarization of the Cu-donor atom bonds. As consequence, the band is an envelope resulted from partial overlapping of three electronic transition bands (table 3) derived from tetragonal splitting of $^2t_{2g}$ and ^2e_g orbital energy levels:$d_{z^2} \rightarrow d_{x^2-y^2}$,$d_{xy}$, $d_{xz} \rightarrow d_{x^2-y^2}$ and $d_{yz} \rightarrow d_{x^2-y^2}$.

The bands centered at 443, 647 and 667 nm was attributed to the M($d_{x^2-y^2}$)-L(π^*) charge transfer transitions, where M is Co(II), Ni(II) and Cu(II), respectively.

From these it could determine that the nitrogen forms with M(II) a bond with higher covalent degree than oxygen, according with Lewis basic hardness of donor-atoms. The shift of n_N-π^* transition is influenced by the compatibility between N-donor ligand and M(II), the steric and electronic effects of the p-nitrobenzyl group.

ESR spectroscopy

The spectrochemical scission factor (g) and the number of impair electrons for each central ion was calculated based on literature (Bhave and Kharat, 1981) according to the following relation:

$$\mathbf{N_x = N_e \frac{(I_x H^2_{max})_x}{(I_e H^2_{max})_c}} \quad (1)$$

where:

- N_x and N_e represents the number of impair electrons of the studied sample and of the standard sample. N_e has the value $0.281 \cdot 10^{20}$ impair electrons mL^{-1};
- I_x and I_e are the signal amplitudes for the analysed and respectively standard sample;
- $(H_{max})_x$ and $(H_{max})_e$ are the intensity values of the maximum magnetic field corresponding to the sample and to the standard.

The g factor is calculated according to the following relation:

$$g = g_e (H_x/H_e) \quad (2)$$

where g_e = 2.0055 for the standard sample. H_x and H_e represent the magnetic field corresponding to the centre of the studied sample spectrum and respectively of the standard H_e = 3216.9 Gauss.

The above relations could be applied when both spectra curves (analysed and standard), are of the same type (Gauss or Lorentz). The *g* value is higher, for the complexes with organic ligands, than that of the free electron and is correlated with the arrangement of the ligands around the central atom. Table 4 presents the values for *g* factor, H_x and the number of impair electrons corresponding to each central atom. It can be observed that all complexes are paramagnetic and with high spin.

Table 4
ESR Parameters for the Synthesised Compounds

Compound	*g*	H_x	Number of impair electrons / central ion
$Mn[(L)_2(H_2O)_2]$	2.0207	3243.00	4.86
$Co[(L)_2(H_2O)_2]$	2.0224	3240.70	2.92
$Ni[(L)_2(H_2O)_2]$	2.0301	3234.90	1.94
$Cu[(L)_2(H_2O)_2]$	2.0223	3237.50	0.94

X-ray diffraction

Table 5 presents the results of X-ray interpretation. From the data presented, it is worth mentioning that all complexes have one side of polyhedron crystallization smaller than the other two, on which side are positioned probably water molecules.

Also the elementary cell volume of all coordination compounds is less than the volume of the elementary cell ligand, which is justified by the nature of the forces that help maintain lattice, molecular for ligand and dipolar for complex combinations.

Table 5
Elementary Cell Parameters of Ligand and Synthesized Compounds

Param.	Ligand (L)	$Mn[(L)_2(H_2O)_2]$	$Co[(L)_2(H_2O)_2]$	$Ni[(L)_2(H_2O)_2]$	$Cu[(L)_2(H_2O)_2]$
α, [º]	111.5130	85.8111	134.3122	35.9750	50.3101
β, [º]	116.8270	93.9395	109.8017	141.6910	47.9812
γ, [º]	105.2380	34.4766	46.2142	139.4510	32.0699
a, [Å]	10.8406	8.7884	9.0333	11.2366	12.1802
b, [Å]	8.4247	10.7573	13.6695	10.8320	12.3776
c, [Å]	7,7871	15.6821	12.9773	18.3642	11.5645
Volume [$Å^3$]	590.0735	814.88	794.6822	764.63	693.6812
System	*triclinic*	*triclinic*	*triclinic*	*triclinic*	*triclinic*

The crystallization system of the compound with Cu(II) differs from the other compounds due to higher volume of copper ion compared to the other divalent ions.

Based on the data presented, a structure of the complex combinations can be obtained, similar to the one in Fig. 4.

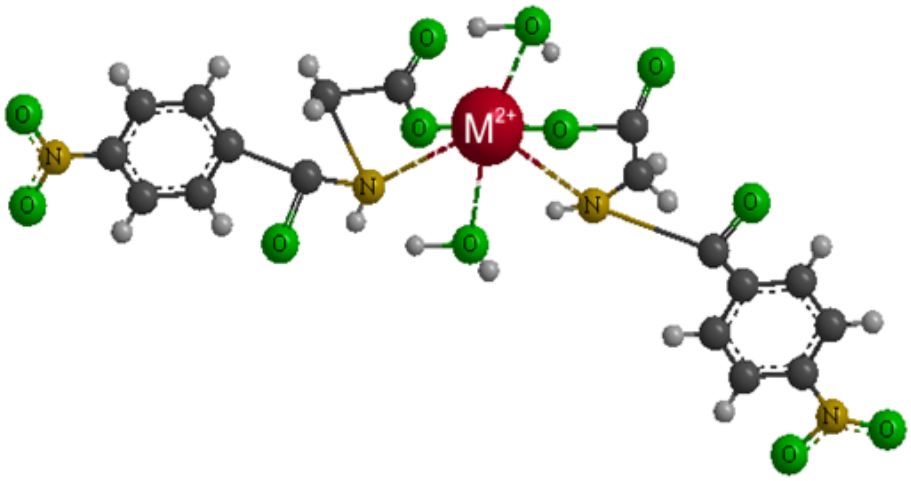

Fig. 4 − Structure complex combinations of type $M[(L)_2(H_2O)_2]$.

Thermal analysis

In a first stage occurs the loss of coordination water molecules:

$$(M(L)_2(H_2O)_2)_{(s)} \xrightarrow{t^0C} (M(L)_2)_{(s)} + 2\ (H_2O)_{(g)} \quad (3)$$

In the second oxidation step occurs the various fragments broken from the organic ligand:

$$(M(L)_2)_{(s)} \xrightarrow{t^0C} B_{(g)} + MO_{(s)} \quad (4)$$

where M is Mn, Co, Ni, Cu and B is a mixture of CO_2, NO_2 and H_2O.

The main parameters of the thermal decomposition process, calculated by the method of (Freeman and Carroll, 1958), are presented in Table 6.

Complexes decompose into three stages except $Ni(L)_2(H_2O)_2$. As mentioned above, in the first stage adsorbed and the coordination water are lost.

In the second stage, due to inductive and electromere effects that occur in the presence metal with low electronegativity (Fig. 5) the chemical bonds breaking occurs between C(1) and N(1) and the oxidation fragment.

In the third stage there is a complete break with the formation of metal oxide.

In the case of the Ni(II) complex, decomposition occurs in four stages, the first water loss, the second about other similar compounds, but steps 3 and 4 are different in terms of losses, probably breaking organic fragments occurs randomly.

Table 6

Thermal Decomposition Process Parameters for Compounds Synthesized

Stage		L	Mn	Co	Ni	Cu
1	A	$1.79x10^{18}$	$1.35x10^{18}$	$8.58x10^{18}$	$1.02x10^{18}$	$5.39x10^{17}$
	Ea / kJ/mol	55.74	94.33	56.41	88.54	53.18
	n	0.98	1.95	0.74	1.9	0.62
	Ti ºC	221.38	46	110.28	49	95.17
	loss%*	58.62	7.74	15.88	7.38	48.88
2	A	an intermediate step slow loss of 15.4%	$1.92x10^{18}$	$4.40x10^{21}$	$6.24x10^{19}$	linear loss of 17.99% from 275.31 C
	Ea / kJ/mol		76.37	60.15	100.53	
	n		1.04	0.86	1.47	
	Ti ºC		201	218.53	223.39	
	loss%*		39.42	38.32	31.22	
3	A	$6.87x10^{20}$	$2.57x10^{21}$	$5.09x10^{20}$	linear loss of 21.0-26.51% from 299ºC	$1.28x10^{18}$
	Ea / kJ/mol	44.32	59.86	62.33		146.84
	n	0.12	0.69	0.67		1.09
	Ti ºC	465	430	431.9		438
	loss%*	25.98	25.73	32.43		20.55
Final residue, [%]**		0	12.94/13.5	13.37/13.78	13.89/13.75	15.01/14.51

*theoretical for $M[(L)_2(H_2O)_2]$ / practical

**theoretical from decomposition to MO / practical

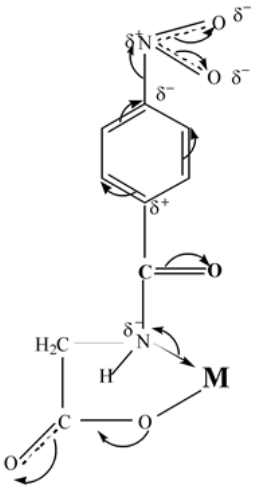

Fig. 5 − Inductive and electromere effects taking place in molecule due generator from complex ligand.

In case of the ligand, without the influence of metal, decomposition takes place in two stages. In the first stage, two benzene cycles break with

oxidation inside organic fragment on the top of C(1), -HN-HC-COOH, (theoretical loss of almost 33.79%, 32.14%), followed in the second stage, by the breakage and benzene oxidation cycles into a continuous phase and a better-defined phase from which kinetic parameters could be calculated.

Toxicity analysis

The acute toxicity resides in the mortality evaluation produced by the contact substance by any kind of administration. The best indication in interpreting the results is given by the dose that kills 50% of the experimental animals (LD_{50}), test that became indispensable for the new substances characterization (Dommer, 1971). Due to the fact that the four compounds could have antitumor action, acting as antimetabolites, the gradual testing of toxicity was performed, and LD_{50} is determined. Mice are the most sensitive animals for the toxicity determination and that is why we used sets of ten animals of 20±2 g, of both sexes with a security limit of 30%. The insoluble in water compounds were suspended in Twen 80 and injected intraperitoneal on a daily basis. The mice were monitored for seven days, determining LD_{50} according to the Spearman – Karber method (Hamilton *et al*., 1978). The obtained results are listed in Table 7 and the main conclusion that can be drawn is that toxicity values are within the limits, which makes it suitable for laboratory screening.

Table 7

The Toxicity Determination of Studied Compounds

Compound	LD_{50}, [mg/kg body]
ligand	6012
$Mn[(L)_2(H_2O)_2]$	5967
$Co[(L)_2(H_2O)_2]$	5923
$Ni[(L)_2(H_2O)_2]$	5970
$Cu[(L)_2(H_2O)_2]$	5997

From the data presented in Table 7, all compounds present low toxicity. Among them, the lowest toxic potential is presented by $Cu[(L)_2(H_2O)_2]$ close to that of the ligand. This result is normal taking into account the literature data, according to which the use of N-acylated amino acids for different combinations positively influence the toxicity degree (Gravatt *et al*., 1994; Moise *et al*., 2008; Moise *et al*., 2009).

Biological activity

Biological screening tests for the ligand and synthesized complexes were carried out against various pathogenic bacteria and fungi species using the agar well diffusion and the tube diffusion methods, respectively (Ashok 1999; Kumar *et al*., 2010; Rahman and Choudhary, 2001). The results are given in Table 8 and 9.

Table 8
Antibacterial Activity Data of Synthesized Compounds

Bacteria	Zone of inhibition, [mm]					
	$Mn[(L)_2(H_2O)_2]$	$Co[(L)_2(H_2O)_2]$	$Ni[(L)_2(H_2O)_2]$	$Cu[(L)_2(H_2O)_2]$	Ligand	Control
E. coli	7	10	6	5	7	-
B. subtilis	22	25	15	19	14	-
St. aureus	11	14	9	7	7	-
P. aeruginosa	24	27	14	19	13	-

Table 9
Antifungal Activity Data of Synthesized Compounds

Fungus	Percent of growth inhibition, [%]					
	$Mn[(L)_2(H_2O)_2]$	$Co[(L)_2(H_2O)_2]$	$Ni[(L)_2(H_2O)_2]$	$Cu[(L)_2(H_2O)_2]$	Ligand	Control
C. albicans	41.9	30.6	15.2	55.7	13.6	-
A. flavus	6.3	4.4	3.5	8.9	1.8	-

All of the synthesized compounds showed significant antibacterial activity against the tested bacteria. The antimicrobial activity of the complexes has been found to decrease in the following order: Ni > Cu >Mn> Co. All the compounds screened are more active against *B. subtilis* and *P. aeruginosa* then the *E. coli* and *St. aureus*. The ligand was found to be less active against the tested bacteria, but plays an important role in determining the degree of the activity of synthesized compounds.

The antifungal activity of N-(p-nitrobenzoyl)-L-phenylglycine derivatives is given in Table 9, which show that the Cu $[(L)_2(H_2O)_2]$ is more active than the Mn, Ni, Co compounds. All the compounds are more active against *Candida albicans* than the *Aspergillus flavus*. The ligand also exhibits good activity, only against *Candida albicans*. Thus, the activity of the synthesized compounds against the tested fungus species was observed to decrease in the following order: Cu>Mn>Co>Ni.

4. Conclusions

Four new compounds of metals: Mn, Co, Ni, Cu with N-(p-nitrobenzoyl)-L-phenylglycine were synthesized and analyzed by various physicochemical methods to establish their structure.

The synthesized compounds showed significant antibacterial activity against the tested bacteria, the more effective being $Co[(L)_2(H_2O)_2]$.

All compounds present moderate toxicity against tested fungi, only $Cu[(L)_2(H_2O)_2]$ present a significantly growth inhibition against *C. albicans* (54.3%).

REFERENCES

Ashok R., *Antifungal Susceptibility Testing*, IJMR, **17**, *3*, 125-128 (1999).

Bhave N.S., Kharat R.B., *Synthesis, Spectral and Magnetic Studies of Co-Ordination Polymers of Co(II), Ni(II), Cu(II) and Pd(II) with 2,6-Dimercaptio-4-Amino-1,3,5-Triazine (DAT)*, J. Inorg. Nucl. Chem, **43**, *2*, 414-426 (1981).

Chen H., Li Z., Han Y., *Synthesis and Fungicidal Activity Against Rhizoctonia Solani of 2-Alkyl(Alkylthio)-5-Pyrazolyl-1,3,4-Oxadiazoles (Thiadiazoles)*, J. Agric. Food Chem., **48**, 5312-5315 (2000).

Dommer E., *Animal Experiments in Pharmacological Analysis*, Charles C. Thomas, Springfield, 283-297, 1971.

Forti L., Menabue L., Saladini M., *Coordination Behaviour of N-Protected Amino Acids. Structural and Spectroscopic Study of Complexes of Co^{II}, Ni^{II} and Cu^{II} with N-(4-Aminobenzoyl)Glycine*, J. Chem. Soc., Dalton Trans., **11**, 2955-2959 (1991).

Freeman E.S., Carroll B., *The Application of Thermoanalytical Techniques to Reaction Kinetics: The Thermogravimetric Evaluation of the Kinetics of the Decomposition of Calcium Oxalate Monohydrate*, J. Phys. Chem., **62**, *4*, 394-397 (1958).

Gokce M., Cakir B., Earl K., Sahin M., *Synthesis and Antimicrobial Activity of [(2-Oxabenzothiazolin-3-Yl)-Methyl]-4-Alkyl/Aryl-1,2,4-Triazoline-5-Thiones*, Arch. Pharm., **334**, 279-283 (2001).

Gravatt G., Baqulez B., Wilson W., Denny W., *DNA-Directed Alkylating Agents. 6. Synthesis and Antitumor Activity of DNA Minor Groove-Targeted Aniline Mustard Analogs of Pibenzimol, (Hoechst 33258)*, J. Med. Chem., **37,** 4338-4345 (1994).

Gudasi K.B., Patil M. S., Vadavi R. S., Shenoy R. V., Patil S. A., Nethaji M., *X-Ray Crystal Structure of Phenylglycine Hydrazide: Synthesis and Spectroscopic Studies of its Transition Metal Complexes*, Spectrochimica Acta Part A: Molecular and Biomolecular Spectroscopy, **67**, *1*, 172-177 (2007).

Hamilton M.A., Russo R.C., Thurston R.V., *Trimmed Sperman-Karber Methode Estimating Median Lethal Concentrations in Bioassays*, Environ. Sci. Technol. **12**, 417-417 (1978).

Hodgson J.B., Percy G.C., Thornton D.A., *Band Assignments in the I.R. Spectrum of Trans-Bis(Glycinato)Platinum(II) by Multiple Isotopic Labelling*, Transition Met. Chem., **4**, 218-220 (1979).

Inomata Y., Shibata A., Yukawa Y., Takeuchi T, Moriwaki T., *The Metal Complexes of Amino Acids and their N-Substituted Derivatives-VII. The i.r. Spectra and Normal Coordinate Analyses of Bivalent Metal Complexes with N-Methylglycine and N-Phenylglycine*, Spectrochimica Acta Part A: Molecular Spectroscopy, **44**, *1*, 97-107 (1988).

Kumar R., Shrivastava S. K., Chakraborti A., *Comparison of Broth Dilution and Disc Diffusion Method for the Antifungal Susceptibility Testing of Aspergillus Flavus*, Am. J. Biomed. Sci., **2**, *3*, 202-208 (2010).

Malek K., Vala M., Swiatek-Kozlowska J., Proniewicz L.M., *Solid State Study of the Copper(II) Complex of 2-Hydroxyiminopropanoic Acid*, New. J. Chem, **28**, 477-483 (2004).

Moise M., Șunel V., Profire L., Popa M., Lionte C., *Synthesis and Antimicrobial Activity of Some New (Sulfon-Amidophenyl)-Amide Derivatives of N-(4-Nitrobenzoyl)-Phenylglycine and N-(4-Nitrobenzoyl)-Phenylalanine*, Farmacia, **56**, 283-289 (2008).

Moise M., Șunel V., Profire L., Popa M., Desbrieres J., Peptu C., *Synthesis and Biological Activity of Some New 1,3,4-Thiadiazole and 1,2,4-Triazole Compounds Containing a Phenylalanine Moiety*, Molecules, **14**, 2621-2631 (2009).

Nakamoto K., *Infrared and Raman Spectra of Inorganic and Coordination Compounds*, John Wiley & Sons, Ltd., 1986.

Pelagatti P., Bacchi A., Calbiani F., Carcelli M., Elviri L., Pelizzi C., Rogolino D., *Inverted Piano-Stool Dimers of Half-Sandwich Ru(II) Complexes with (R)-Phenylglycine Methylester and (S)-Phenylalanineamide: An X-Ray Structural Study and Preliminary Catalytic Results*, Journal of Organometallic Chemistry, **690**, 21-22, 4602-4610 (2005).

Pintilie O., Moise M., Profire L., Șunel V., *Synthesis and Biological Activities of Some Beta-Lactamic Derivatives*, Farmacia, **54**, *61*, 61-69 (2006).

Pintilie O., Profire L., Șunel V., Popa M., Pui A., *Synthesis and Antimicrobial Activity of Some New 1,3,4-Thiadiazole and 1,2,4-Triazole Compounds Having a D,L-Methionine Moiety*, Molecules, **12**, 103-113 (2007a).

Pintilie O., Șunel V., Profire L., Pui A., *Synthesis and Antimicrobial Activity of Some New (Sulfonamidophenyl)-Amides of N-(Metanitrobenzoyl)-D,L-Methionine*, Farmacia, **55**, 345-251 (2007 b).

Rahman A., Choudhary M.I., Thomsen W.J., *Bioassay Techniques for Drug Development*, Harward Academic Press, Amsterdam, **14** (2001).

Ryabov A.D., Polyakov V.A., Yatsimirsky A.K., *Some Complexes of Palladium(II) with C-Phenylglycine and its Derivatives. Cyclopalladation of N,N-Dimethyl-C-Phenylglycine Ethyl Ester*, Inorganica Chimica Acta, **91**, *1*, 59-65 (1984).

Salas Peregrin J.M., Rodriguez E.C., Valera J.S., Avila Roson J.C., *Synthesis, Characterization and Thermal Behaviour of Some N-2,3-Dimethyl-Phenylglycine Compounds of Al(III), Mn(II), Fe(III), Y(III), Cd(II), La(III), Ce(III) and Pb(II)***,** Thermochimica Acta, **95**, *1*, 111-118 (1985).

Șunel V., Lionte C., Băsu C., Cheptea C., *New Antitumour Alkylating Compounds with N-[m-(Arylthiocarbamoyl)-Aminobenzoyl]-Asparagic Acids Support*, Chem. Indian J., **2**, 1-6 (2005).

Șunel V., Popa M., Desbrieres J., Profire L., Pintilie O., Lionte C., *New di-(β-Chloroethyl)-α-Amides on N-(m-Acylaminobenzoyl)-D, L-Aminoacid Supports with Antitumoral Activity*, Molecules, **13**, 177-189 (2008).

Șunel V., Lionte C., Popa M., Pintilie O., Mungiu P., Teleman S., *Synthesis of New Methionine Derivatives for the Treatment of Paracetamol-Inducet Hepatic Injury*, Eur. Chem. Tech. J., **4,** 201-205 (2002).

Varvarason A., Tantili-Kakoulidou A., Siatra-Papastasikoudi T., Tiligada E., *Synthesis and Biological Evaluation of Indole Containing Derivatives of Thiosemicarbazide and their Cyclic 1,2,4-Triazole and 1,3,4-Thiadiazole Analogs*, Arzneim. Forsch., **50**, 48-54 **(**2000).

Zamani K., Faghifi K., Tefighi I., Sharlatzadeh R., *Synthesis and Potential Antimycotic Activity of 4-Substituted 3-(Thiophene-2-Yl-Methyl)-Δ2-1,2,4-Triazoline-5-Thiones*, Turk. J. Chem., **28**, 95-101 (2004).

Zan X.I., Lai L.H., Jin G.Y., Zhong Z.X., *Synthesis, Fungicide Activity and 3D- QSAR of 1,3,4-Oxadiazoles and 1,3,4-Thiadiazoles*, J. Agric. Food Chem, **50**, 3757-3760 (2002).

SINTEZA, CARACTERIZAREA ŞI ANALIZA TOXICITĂŢII UNOR COMPLECŞI DIVALENŢI DE METALE TRANZIŢIONALE CU N-(p-NITROBENZOIL)-L-GLICINĂ

(Rezumat)

Această lucrare prezintă sinteza, caracterizarea structurală şi fizico-chimică a unor combinaţii complexe ale Mn(II), Co(II), Ni(II) şi Cu(II) cu N-(p-nitrobenzoil)-L-glicină ca ligand. S-au sintetizat patru combinaţii complexe în raport molar 1:2, urmată de caracterizarea şi determinarea potenţialului lor toxic (doza letală de toxicitate), precum şi analiza unor proprietăţi antifungice şi antibacteriene. Etapa de caracterizare implică determinarea structurii, care a fost efectuată prin analiza elementară, spectroscopia FTIR, XRD, rezonanţa electronică de spin (ESR) şi stabilitatea termică. Datele experimentale arată că toţi compuşii au o structură cristalină (sistem ortorombic) şi sunt stabili termic până la temperaturi de peste 100°C. Testele de toxicitate ale compuşilor noi s-au desfăşurat pe şoareci şi rezultatele indică faptul că cea mai mică valoare a dozei letale o are compusul de cupru. Activităţile biologice şi antifungice au fost investigate pentru toţi compuşii. Compusul cu cobalt prezintă cele mai bune proprietăţi antibacteriene, iar compusul de cupru prezintă cele mai bune proprietăţi antifungice.